A&A 503, 991–997 (2009)
DOI: 10.1051/0004-6361/200912066

Astronomy & Astrophysics

Coronal hole boundaries evolution at small scales

I. EIT 195 Å and TRACE 171 Å view⋆

M. S. Madjarska[1,2] and T. Wiegelmann[1]

[1] Max-Planck-Institut für Sonnensystemforschung, Max-Planck-Str. 2, 37191 Katlenburg-Lindau, Germany
[2] Armagh Observatory, College Hill, Armagh BT61 9DG, N. Ireland
e-mail: madj@arm.ac.uk

Received 13 March 2009 / Accepted 4 June 2009

ABSTRACT

Aims. We aim to study the small-scale evolution at the boundaries of an equatorial coronal hole connected with a channel of open magnetic flux to the polar region and an "isolated" one in the extreme-ultraviolet spectral range. We determine the spatial and temporal scale of these changes.
Methods. Imager data from TRACE in the Fe IX/X 171 Å passband and EIT on-board Solar and Heliospheric Observatory in the Fe XII 195 Å passband were analysed.
Results. We found that small-scale loops known as bright points play an essential role in coronal hole boundary evolution at small scales. Their emergence and disappearance continuously expand or contract coronal holes. The changes appear to be random on a time scale comparable to the lifetime of the loops seen at these temperatures. No signature was found for a major energy release during the evolution of the loops.
Conclusions. Although coronal holes seem to maintain their general shape during a few solar rotations, a closer look at their day-by-day and even hour-by-hour evolution demonstrates significant dynamics. The small-scale loops (10″–40″ and smaller) which are abundant along coronal hole boundaries contribute to the small-scale evolution of coronal holes. Continuous magnetic reconnection of the open magnetic field lines of the coronal hole and the closed field lines of the loops in the quiet Sun is more likely to take place.

Key words. Sun: atmosphere – Sun: corona – methods: observational – methods: data analysis

1. Introduction

Coronal holes (CHs) are large regions on the Sun that are magnetically open. They are identified as the source of the fast solar wind (~800 km s^{-1}) (Krieger et al. 1973) and are visible in coronal lines (formed at temperatures above 6×10^5 K) as regions with a reduced emission relative to the quiet Sun (Wilhelm 2000; Stucki et al. 2002). There are two types of coronal holes: polar and mid-latitude CHs. During the minimum of solar activity, the solar atmosphere is dominated by two large CHs situated at both polar regions. The mid-latitude CHs can be either "isolated" or connected with a channel of open magnetic flux to a polar CH. The latter are called equatorial extensions of polar CHs (EECHs). The isolated coronal holes have an occurrence rate that follows the solar activity cycle and are usually connected with an active region (Insley et al. 1995).

Huber et al. (1974) compared the appearance and physical parameters of the different layers of the solar atmosphere in and outside coronal holes (e.g. the quiet Sun) using the Apollo Telescope mount on Skylab. Their measurements of the height of emission of various ions at different ionisation stages (different formation temperatures) at the polar limb indicated an increase of the thickness of the transition region underlying coronal holes. Hence, they found a difference between quiet Sun and coronal holes already pronounced at transition region temperatures.

Feldman et al. (1999) studied the morphology of the upper solar atmosphere using high-resolution data (1″–2″) taken by the transition region and corona explorer (TRACE), solar ultraviolet measurements of emitted radiation spectrometer (SUMER) on-board SoHO and the Naval Research Laboratory spectrometer on Skylab. The authors found that in the temperature range 4×10^4 K $\leq T_e \leq 1.4 \times 10^6$ K, the upper solar atmosphere is filled with loops of different sizes with hotter and longer loops overlying the cooler and shorter loops (Dowdy et al. 1986). At heights above 2.5×10^4 km in the upper solar atmosphere of the quiet Sun, only loops at temperatures $T_e \sim 1.4 \times 10^6$ K exist. No distinction was found between quiet Sun and coronal hole morphology at $5 \times 10^4 \leq T_e \leq 2.6 \times 10^5$ K. This suggests that both regions are filled with structures of similar sizes which are emitting at similar temperatures. These structures do not exceed a height of 7 Mm and have lengths ≤21 Mm. Feldman et al. (1999) also investigated the coronal hole boundaries concluding that they are seeded with small-scale loops (<7 Mm). There coexist, however, long loops at temperatures above $T \sim 1.4 \times 10^6$ K which generally originate from the same location but close to faraway locations.

Wiegelmann & Solanki (2004) made a further step by reconstructing the magnetic field in coronal holes and the quiet Sun with the help of a potential field model. They found that the CH loops are on average shorter, lower and flatter than in the QS. High and long closed loops are extremely rare in CHs, whereas short and low loops are almost as abundant as in the

⋆ Movies are only available in electronic form at http://www.aanda.org

QS region. This result strongly supports the observational findings on the structure of the upper solar atmosphere in the quiet Sun and coronal holes.

Based on Skylab data in soft X-rays, Timothy et al. (1975) first reported the distinctive feature of the EECHs to exhibit quasi-rigid rotation. Shelke & Pande (1985) found that equatorial CHs (without dividing them in different classes) have a rotational period which is a function of latitude and thus exhibit differential rotation. Navarro-Peralta & Sanchez-Ibarra (1994) showed that isolated CHs have a typical differential rotation, while EECHs maintain two types of rotation rates: differential below a latitude of 40°, which becomes almost rigid when approaching the poles. Insley et al. (1995) concluded that mid-latitude CHs rotate more rigidly than the photosphere, but still exhibit significant differential rotation.

Due to the different rotation profiles at a coronal and photospheric level and the fact that CH boundaries (CHBs) separate two topologically different (open and closed) magnetic field configurations, CHBs are presumably the regions where processes take place that open and close magnetic field lines. The reconfiguration of the CHBs is believed to happen through magnetic reconnection between the open and closed magnetic field lines of the CH and the surrounding quiet Sun.

The small-scale evolution of CH boundaries has been a subject of several studies during the last few decades (Kahler & Moses 1990, and the references therein). These studies aimed at understanding the general evolution of coronal holes, the quasi-rigid rotation of EECH compared to the differentially rotating solar photosphere as well as their relation to the slow solar wind generation. Kahler & Moses (1990) studied Skylab X-ray images of a single EECH with a time resolution of 90 min to look for discrete changes of the CH boundaries. They found that X-ray bright points (BPs, small-scale loops in the quiet Sun and CHs, for details see Madjarska et al. 2003) play an important role in both the expansion and contraction of the CH. For this study, a single coronal hole observed during the decreasing phase of the solar cycle activity was used. Bromage et al. (2000) reported that small-scale changes of the boundaries of the CH on 1996 August 26 took place on time-scales of a few hours in observations with the EIT in Fe XII 195 Å. The authors, however, do not give any details of the nature of these changes. Kahler & Hudson (2002) made the first systematic morphological study of the boundaries of coronal holes as viewed in soft X-ray images from the Yohkoh Soft X-ray telescope. They studied three coronal holes during several rotations, all formed during the maximum of solar activity cycles 23 and 24. All three coronal holes represent equatorial extensions of polar coronal holes. They found that the CHs evolve slowly, and neither large-scale transient X-ray events nor coronal bright points appeared significant factors in the development of CH boundaries. They suggested that open-close magnetic field reconnection is more likely to describe the actual physics at the CHBs. The visibility of BPs in X-ray images is strongly diminished during solar maximum activity by the presence of active regions and bright loops seen in X-rays. The number and size of BPs, and also their lifetime, strongly depend on the temperature at which they are observed, with more and longer living BPs seen in spectral lines formed at lower temperatures.

The emergence of magnetic fields in active regions and their subsequent diffusion due to random convective motions in the photosphere influenced by the meridional flow is believed to be the main mechanism leading to the formation of coronal holes. Wang & Sheeley (1994) developed a model where the footpoint exchange between open and closed magnetic field lines (the socalled "interchange reconnection") generates coronal holes and maintains their quasi-rigid rotation against the differentially rotating photospheric layers. This type of reconnection results in an exchange of footpoints between open and closed magnetic field lines with no change in the total amount of open or closed flux (Wang & Sheeley 1994). The reconnection takes place very high in the corona ($r \sim 2.5\ R_{\odot}$) and occurs continuously in the form of small, stepwise displacements of field lines. According to the authors, this scenario may explain why no X-ray signatures have been detected in association with boundary evolution in long-lived coronal holes studied by Kahler & Hudson (2002). They proposed that the blobs emitted from the tops of helmet streamers as radially elongated density enhancements and associated with the slow solar wind are probably the result of this reconnection process.

Our study aims at providing for the first time an analysis of the small-scale (determined by the instrument resolution) evolution of coronal hole boundaries on a time scale from tens of minutes to hours using EUV (EIT/195 Å and TRACE/171 Å) observations with a spatial resolution ranging from 1″ (TRACE) to 5.5″ (EIT). In Sect. 2 we describe the observational material and data reduction applied. Section 3 presents the data analysis and the obtained results. The discussion and conclusions on the obtained results in the light of the existing theoretical models as well as the future perspectives are given in Sect. 4.

2. Observational material and data reduction

We studied two coronal holes, one observed in October 1996 (hereafter CH1) and the second in November 1999 (hereafter CH2). The CH1 is the well known "Elephant trunk coronal hole", an equatorial extension of a north pole CH which has been the subject of several studies (Bromage et al. 2000, and the references therein). CH2 is an "isolated" mid-latitude CH observed in November 1999. Figure 1 shows EIT images in the 195 Å passband with boxes over-plotted outlining the analysed FOVs for both CHs.

2.1. EIT

The CH1 data were recorded with EIT in the 195 Å passband on 1996 October 19−20 with a full resolution of 2.6″. The images were taken from 20:00 UT (19 October) until 06:00 UT (20 October) every 15 min (except at 05:00 UT). Additionally, we selected full-disk data covering 48 h of observations from 15:00 UT on October 18 until 15:41 UT on October 20 taken approximately every 2 h. All data related to CH1 were derotated to 07:00 UT on October 20. The data from November 1999 were taken from 15:00 UT on November 3 until 15:00 UT on November 5 and de-rotated to 15:00 UT on November 5. Both datasets have a 5.2″ angular pixel size.

The necessary data reduction was applied, i.e. the images were background subtracted, degridded, flat-fielded, degradation corrected and normalised. They were also derotated to a reference time using the drot_map.pro procedure from SolarSoft. The procedure applies synodic values for the differential rotation. Cosmic ray removal was not applied because it was not needed and carries the risk of removing real small-scale structures.

2.2. TRACE

The TRACE data were obtained in Fe IX/X 171 Å on November 4, 1999. The data have a 3 s cadence and a

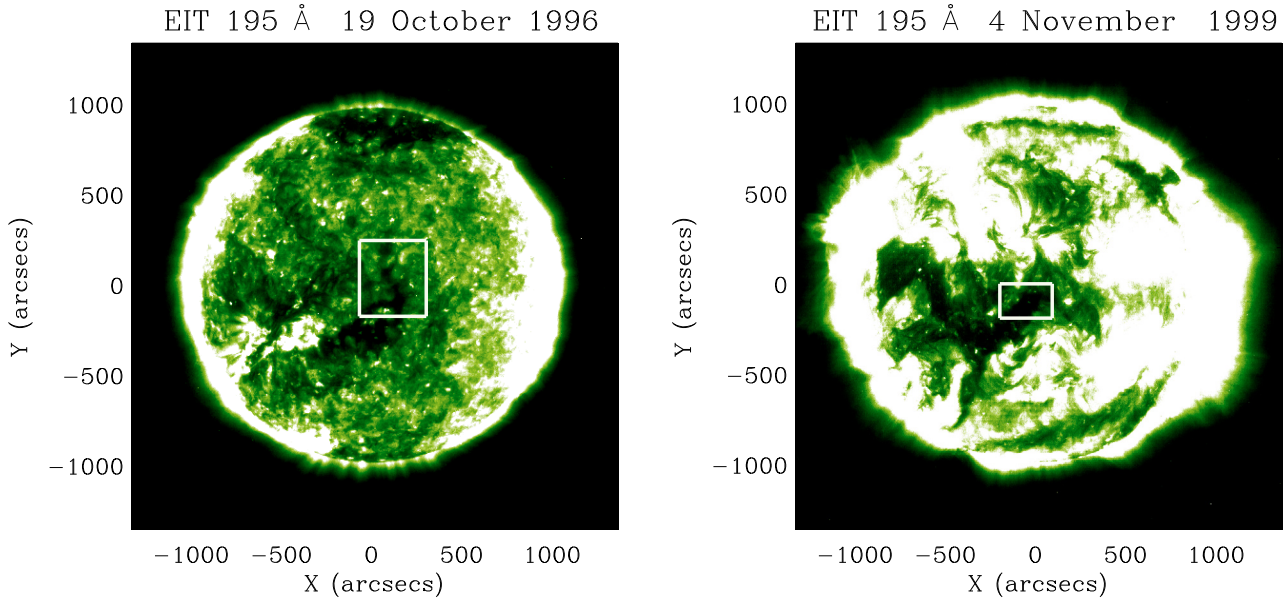

Fig. 1. Full-disk EIT 195 Å images obtained on 1996 October 19 and 1999 November 4. The over-plotted boxes outline the field-of-views subjected to detailed study.

variable exposure time from 00:50 UT to 07:11 UT for approximately 7 h.

The following corrections were applied: dark current subtraction (obtained the day before), flat-field corrections, spike and streak removal. The background diffraction pattern was removed but some residual effects remained. A normalisation for exposure and a pointing offset correction for the studied channel were also applied.

The data were obtained close to the eclipse period (which started on November 7) during which TRACE was attenuated by the Earth atmosphere in parts of its orbit, and the response in the EUV channels is compromised. However, for several weeks either side of the eclipse period, the data are also contaminated. As our data were taken only 3 days before the eclipse started, we had to reduce the number of images used to only 6 (from 434). The images were selected after a careful flux analysis and we are confident that they can be used for the purposes of this study (see later in the text).

In both imagers (EIT and TRACE) the measured values are in data numbers (DN). Data number is the output of the instrument electronics which corresponds to the incident photon signal converted into charge within each CCD pixel. The contours were smoothed in order to remove changes due to image irregularities which could be artifactual changes.

3. Data analysis and results

In the present work we paid special attention to the data reduction in order to get reliable information on the evolution of CH boundaries using a contour plot. This method is more reliable than a visual inspection and ensures the detection of any small-scale changes. The contours have different values for the data with different resolution. The contour values also depend on the observed temperatures, with coronal holes expanding at higher temperatures (Bromage et al. 2000). For the present study, we determined the boundaries as the region that has intensities 1.5 times the average intensity of the darkest region inside the coronal hole. The visual inspection showed that this value describes the boundaries well as determined using He I 10 830 Å images from Kitt Peak National Observatory (Henney & Harvey 2005). For the TRACE 171 Å images of CH2, we used an EIT image obtained in Fe XII 195 Å in order to establish the CHBs. The Fe IX/X 171 Å passband has a transition region emission contribution and is, therefore, not well suited to determine CHBs. We selected two images (EIT and TRACE) obtained at the same time, applied the necessary offset correction, over-plotted the boundaries on the TRACE images as determined by EIT and then established for TRACE its own contour of constant flux which matches well the EIT contour.

In order to follow the evolution of the CHs for the longest possible period of time we produced movies from full-disk images obtained with EIT in the 195 Å passband. An important issue in analysing these images was the projection effect of loops at the CHBs which can mimic changes that are not real. To avoid this problem, we have chosen images showing the CHs with the eastern and western boundaries not further than −300″ and 300″ from the disk center, respectively. The movies can be seen online as movie_1996.mp4 (CH1) and movie_1999.mp4 (CH2). The animated sequences show derotated images of the coronal holes with their boundaries outlined with a solid line. A dashed-dotted line contour corresponds to the first image of the sequence.

Following the CH boundary evolution during 48 h we see significant dynamics related to the evolution of the small-scale loops known as BPs. BPs represent ≈10″−40″ features with enhanced intensity. Their appearance is dependent on the spatial resolution of the instrument, so they are often seen as a bright core surrounded by a diffuse cloud. High-resolution observations (1″−2″) show that BPs consist of several small loops (Sheeley & Golub 1979; Ugarte-Urra et al. 2004; Pérez-Suárez et al. 2008). Only BPs which are close to the CHBs play a role in the expansion or contraction of the CHs. We do not identify any flaring events related to this evolution. For the narrow CH1, the emergence, evolution and disappearance of BPs results in some cases in a complete displacement of parts of the CH in either an eastern or western direction (see the CH1 movie). Madjarska et al. (2004) analysed SUMER spectral lines taken along a part of the

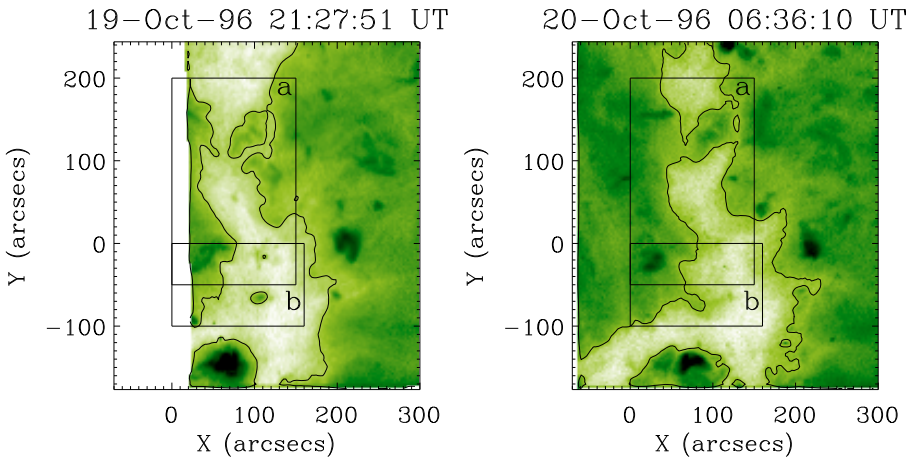

Fig. 2. Color table reversed EIT 195 Å images of the coronal hole observed on October 19−20, 1996. The over-plotted rectangular areas (**a)** and **b)**) are shown enlarged in Figs. 3 and 4.

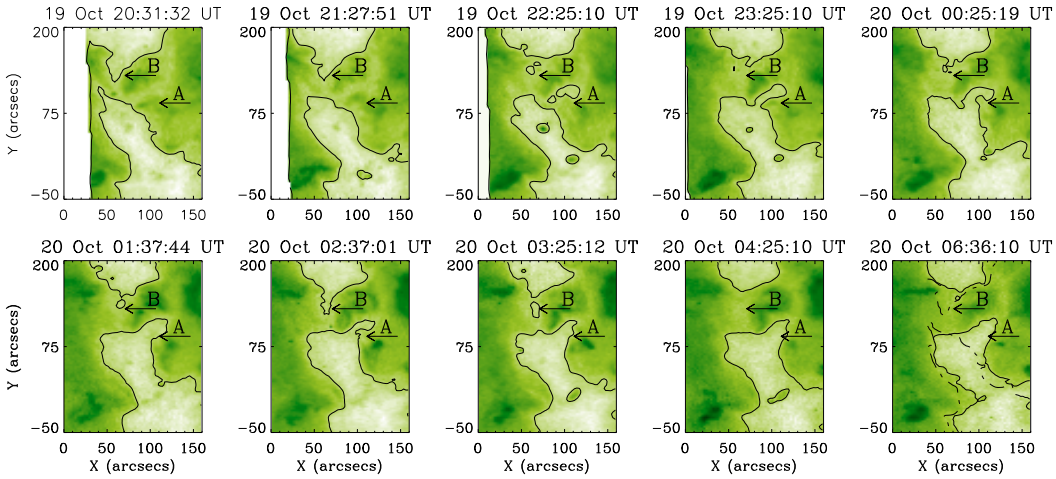

Fig. 3. EIT images of the area marked with "a" in Fig. 2 (reversed color table). The arrows point to the BPs whose evolution led to the expansion (arrow A) and the contraction (arrow B) of the CH. The over-plotted dashed-dotted line shows the boundary from the first image.

CH1. The authors found numerous transient features called explosive events located along the CH boundaries as well as around the BP which is inside the CH (Fig. 1). We also observe displacements of the boundaries which are not related to any clearly distinguishable structure in EIT 195 Å or TRACE 171 Å. A check on temporally close images taken in the EIT He 304 Å ($T \sim 4 \times 10^4$ K) channel clearly shows the existence of a BP that apparently has a low temperature and therefore cannot be seen in the hotter passbands. The time scale of the changes is defined by the lifetime of the BPs which is around 20 h in EUV at coronal temperatures (Zhang et al. 2001) and 8 h in X-rays (Golub et al. 1974).

The next step in our analysis was to study individual cases of evolving loop structures (BPs) and their contribution to the coronal hole evolution in more detail. The analysed FOV for CH1 is shown in Fig. 2 by two images taken at two different times. The two overplotted rectangular boxes (a and b) are shown enlarged in Figs. 3 and 4. The two arrows (A and B) in Fig. 3 are pointing to loop structures (i.e. BPs) whose evolution led to a change of the boundary. In Fig. 3 arrow A shows the disappearance of a BP associated with an expansion of the coronal hole while arrow B indicates the appearance of a loop structure which led to a contraction of the CH. These changes correspond to the size of the evolving BPs. In Fig. 4 a BP evolution is followed by a contraction of the CH.

The CH2 is presented in Fig. 5 with images taken at almost regular time intervals (e.g. 01:12, 02:00, 02:50, 03:38, 05:15 and 06:49 UT). The two over-plotted boxes (a and b) have the enlarged FOV shown in Figs. 6 and 7. In Fig. 6 one can see that formation of a new BP (arrow A) led to contraction of the CH while the disappearance (arrow B) again expanded the CH. In Fig. 7 the disappearance of two BPs is followed by a large increase of the CH region.

4. Discussion and conclusions

The major objective of our study was to determine the dynamics of coronal hole boundaries as seen in the EUV spectral range. To our knowledge, similar studies have only been made in the X-ray spectral domain (Kahler & Moses 1990; Kahler & Hudson 2002), which is sensitive to plasma emitting at temperatures above 3 MK. The examples selected for this study represent an equatorial extension of a polar coronal hole that existed for 4 solar rotations (during the studied rotation the connection was closed above 40°) and an "isolated" coronal hole. Although the coronal holes seem to maintain their general shape for a few solar rotations, a closer look at their day-by-day and even hour-by-hour evolution demonstrates significant dynamics. We found that small-scale loops (30″−40″), which are abundant along coronal hole boundaries at temperatures up to

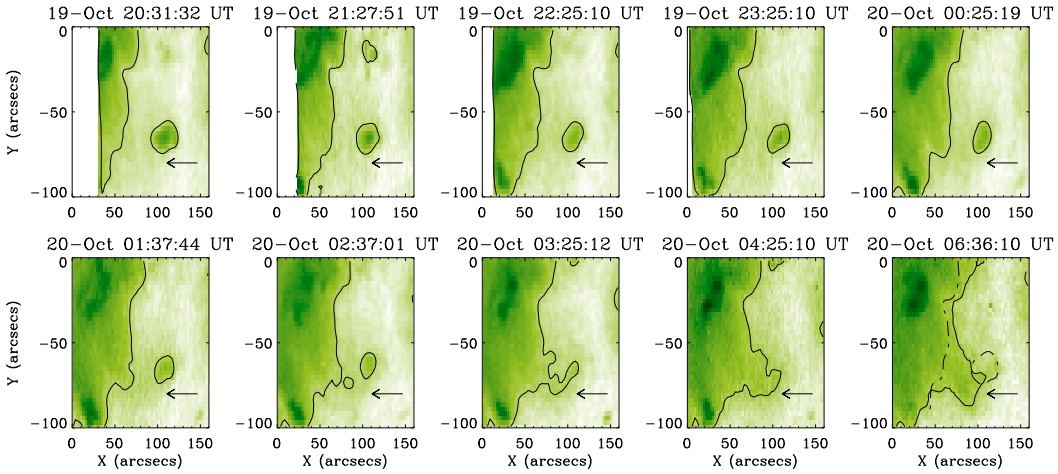

Fig. 4. EIT images of the area marked with "b" in Fig. 2 (reversed color table). The arrows point to a bright point whose evolution led to the contraction of the coronal hole. The over-plotted dashed-dotted line shows the boundary from the first image.

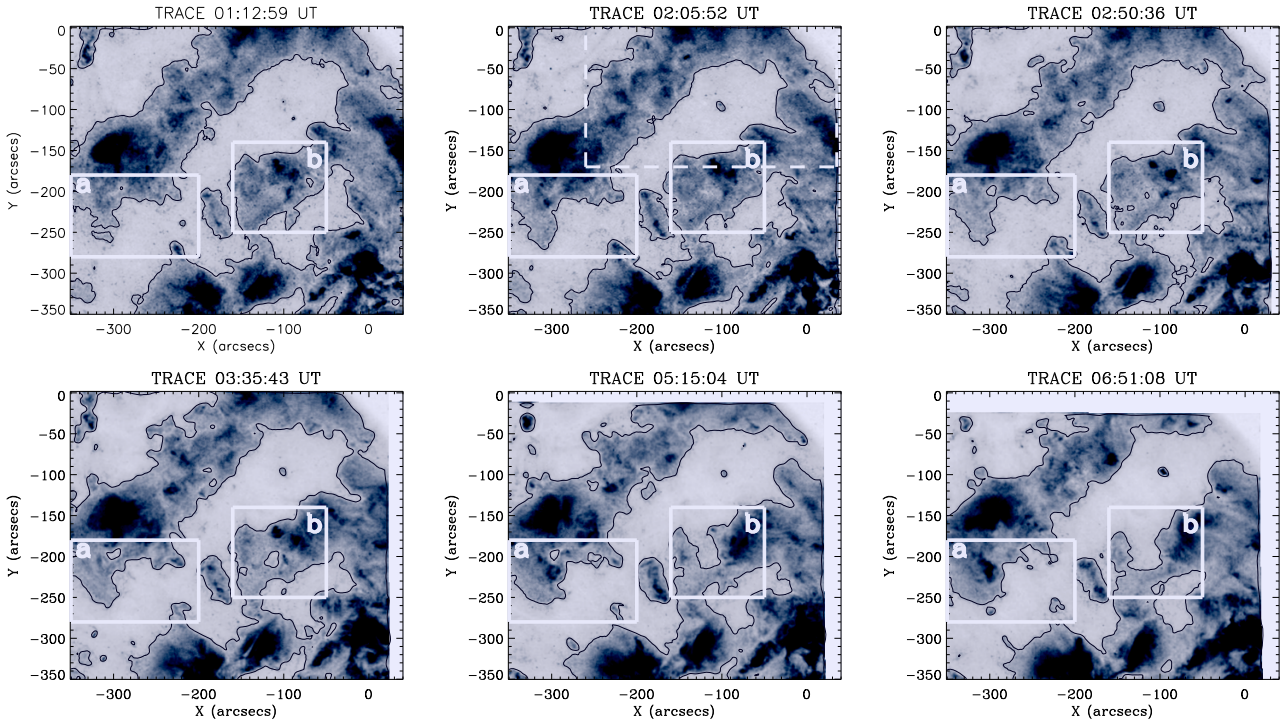

Fig. 5. Reversed color TRACE 171 Å images showing a partial field-of-view of CH2 observed in November 1999. The over-plotted rectangular areas (a and b) are shown enlarged in Figs. 6 and 7. The dashed line box corresponds to the field-of-view presented in Fig. 8.

$T \sim 1.2{-}1.4 \times 10^6$ K, have a major contribution to the evolution of coronal holes. The loop (BP) emergence, evolution and disappearance lead to a continuous expansion or contraction of the coronal holes. In some cases, that can result in closing a narrow coronal hole or a large shift of the entire CH. These changes appear to be random, probably defined by photospheric processes such as convective motion, meridional flow, differential rotation, emergence of magnetic flux as well as intensive inflow of unipolar magnetic flux from attached active region(s). This most probably triggers intensive magnetic reconnection of the closed magnetic field lines of the quiet Sun and the open filed lines of the coronal hole. The spectroscopic study of CH1 by Madjarska et al. (2004) found evidence for magnetic reconnection processes happening at transition region temperatures along the CH1 boundaries, which strongly supports the results of the present work.

How does the appearance and disappearance of BPs transform the boundaries of the coronal holes? We know so far that 88% of X-ray BPs are associated with converging magnetic polarities (Webb et al. 1993) and most of the BPs are related to cancelling magnetic features. Usually, one of the magnetic polarities involved is stronger than the other (Madjarska et al. 2003) and after the full cancellation of the weaker polarity, the remnant one either joins the CH dominant polarity (if it is of the same sign), expanding the CH surface, or forms a new connection (closed magnetic field lines) which triggers contraction of the CH boundaries. This scenario will be tested by applying magnetic field extrapolation on Michelson Doppler Imager data in high-resolution mode for CH2 as well as new

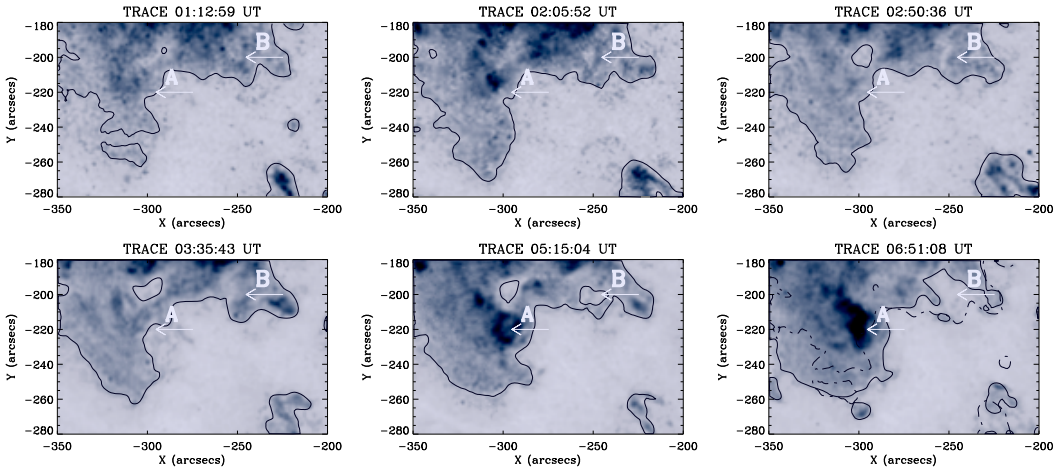

Fig. 6. TRACE 171 Å images marked with "a" in Fig. 5 and showing a contraction of the CH due to the formation of a new BP (arrow A) close to the CH boundary and an expansion due to the disappearance of a BP (arrow B). The over-plotted dashed-dotted line shows the boundary from the first image.

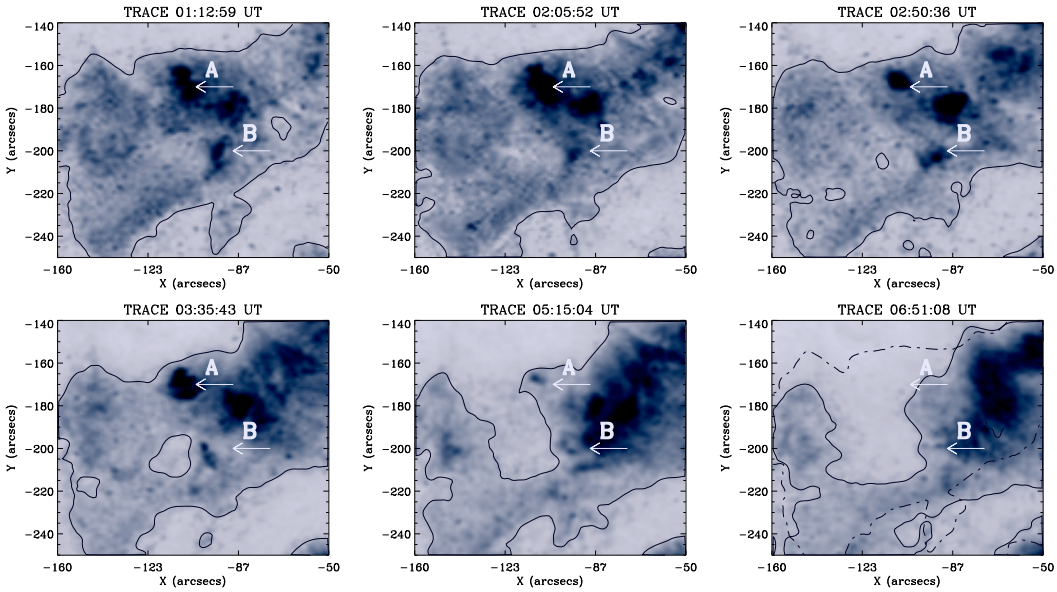

Fig. 7. TRACE 171 Å images marked with "b" in Fig. 5 showing a large expansion of the coronal hole due to the disappearance of two BPs (arrows A and B). The over-plotted dashed-dotted line shows the boundary from the first image.

forthcoming data from SOT/Hinode. An example with potential field extrapolations from SOHO/MDI is shown in Fig. 8. In the future we plan to study the connection between the magnetic and thermal boundary of coronal holes in more detail with the help of extrapolations from full disk magnetograms from SDO/HMI, which will provide the global topology of the coronal magnetic field and allow us to distinguish clearly between globally open and closed regions. The temporal evolution of the fine structure at the coronal hole boundary can be studied with higher resolution and good signal to noise vector magnetograms from Hinode/SOT. In principal, it would be useful also to use more sophisticated magnetic field models than the potential field used here. It is well known that the nonlinear force-free approach is superior for modelling active regions, but unfortunately this approach might not be fully appropriate for coronal hole and quiet Sun regions, due to the finite beta plasma in the quiet sun (Schrijver & van Ballegooijen 2005). Consequently, one should model the magnetic field and plasma self-consistently, in lowest order with a magneto-hydro-static model as described in Wiegelmann & Neukirch (2006). Such an approach is also assumed to automatically provide consistency between thermal and magnetic boundaries of coronal holes. We believe that possible differences between thermal (as identified in EUV images) and magnetic hole boundaries might be an artefact of using too simple magnetic field models.

How do our results contribute to the understanding of the mechanism maintaining the rigid rotation of the equatorial extension of coronal holes? The rotation of coronal holes is usually determined by measuring their centers during several rotations e.g. determining their Carrington longitude from rotation to rotation (Navarro-Peralta & Sanchez-Ibarra 1994). These measurements, however, do not take into account the small-scale evolution of coronal holes. Our analysis shows that especially in the case of narrow coronal holes the open magnetic flux could be totally "recycled" (Close et al. 2004, 2005) by the continuous interaction with the closed magnetic flux and therefore in the subsequent rotation, the appearance of the coronal hole will be the result of complex changes. An example is CH1 which

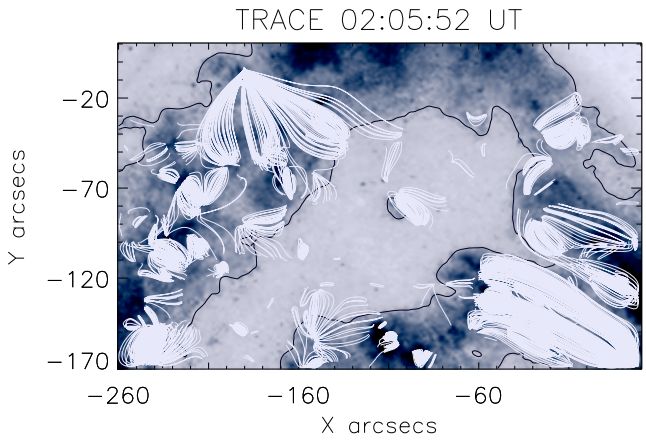

Fig. 8. TRACE 171 Å image with a field-of-view as shown in Fig. 5 with over-plotted only closed magnetic field lines connecting magnetic polarities above 20 G. The magnetic field lines were obtained with a potential magnetic field extrapolation (Wiegelmann et al. 2005).

almost completely disappeared in September 1996 and reappeared again in November 1996.

New studies based on specially designed and completed observing programs with SUMER/SoHO, EIS, XRT and SOT/Hinode and TRACE during the last two years, are ongoing and will present the XRT/Hinode view (Paper II) and EIS and SUMER view (Paper III). These works should reveal more on the physical nature of the reported changes as well as a possible relation between the activity along the coronal hole boundaries and the origin of the slow solar wind.

Acknowledgements. M.M. thanks ISSI, Bern for the support of the team "Small-scale transient phenomena and their contribution to coronal heating". Research at Armagh Observatory is grant-aided by the N. Ireland Department of Culture, Arts and Leisure. We also thank STFC for support via grants ST/F001843/1 and PP/E002242/1. The work of TW was supported by DRL-grant 50 OC 0501. SoHO is a mission of international collaboration between ESA and NASA.

References

Bromage, B. J. J., Alexander, D., Breen, A., et al. 2000, Sol. Phys., 193, 181
Close, R. M., Parnell, C. E., Longcope, D. W., & Priest, E. R. 2004, ApJ, 612, L81
Close, R. M., Parnell, C. E., Longcope, D. W., & Priest, E. R. 2005, Sol. Phys., 231, 45
Dowdy, Jr., J. F., Rabin, D., & Moore, R. L. 1986, Sol. Phys., 105, 35
Feldman, U., Widing, K. G., & Warren, H. P. 1999, ApJ, 522, 1133
Golub, L., Krieger, A. S., Silk, J. K., Timothy, A. F., & Vaiana, G. S. 1974, ApJ, 189, L93
Henney, C. J., & Harvey, J. W. 2005, in Large-scale Structures and their Role in Solar Activity, ed. K. Sankarasubramanian, M. Penn, & A. Pevtsov, ASP Conf. Ser., 346, 261
Huber, M. C. E., Foukal, P. V., Noyes, R. W., et al. 1974, ApJ, 194, L115
Insley, J. E., Moore, V., & Harrison, R. A. 1995, Sol. Phys., 160, 1
Kahler, S. W., & Hudson, H. S. 2002, ApJ, 574, 467
Kahler, S. W., & Moses, D. 1990, ApJ, 362, 728
Krieger, A. S., Timothy, A. F., & Roelof, E. C. 1973, Sol. Phys., 29, 505
Madjarska, M. S., Doyle, J. G., Teriaca, L., & Banerjee, D. 2003, A&A, 398, 775
Madjarska, M. S., Doyle, J. G., & van Driel-Gesztelyi, L. 2004, ApJ, 603, L57
Navarro-Peralta, P., & Sanchez-Ibarra, A. 1994, Sol. Phys., 153, 169
Pérez-Suárez, D., Maclean, R. C., Doyle, J. G., & Madjarska, M. S. 2008, A&A, 492, 575
Schrijver, C. J., & van Ballegooijen, A. A. 2005, ApJ, 630, 552
Sheeley, Jr., N. R., & Golub, L. 1979, Sol. Phys., 63, 119
Shelke, R. N., & Pande, M. C. 1985, Sol. Phys., 95, 193
Stucki, K., Solanki, S. K., Pike, C. D., et al. 2002, A&A, 381, 653
Timothy, A. F., Krieger, A. S., & Vaiana, G. S. 1975, Sol. Phys., 42, 135
Ugarte-Urra, I., Doyle, J. G., Madjarska, M. S., & O'Shea, E. 2004, A&A, 418, 313
Wang, Y.-M., & Sheeley, Jr., N. R. 1994, ApJ, 430, 399
Webb, D. F., Martin, S. F., Moses, D., & Harvey, J. W. 1993, Sol. Phys., 144, 15
Wiegelmann, T., & Neukirch, T. 2006, A&A, 457, 1053
Wiegelmann, T., & Solanki, S. K. 2004, Sol. Phys., 225, 227
Wiegelmann, T., Xia, L. D., & Marsch, E. 2005, A&A, 432, L1
Wilhelm, K. 2000, A&A, 360, 351
Zhang, J., Kundu, M. R., & White, S. M. 2001, Sol. Phys., 198, 347